

# Flame Retardancy and Thermal Degradation Behavior of Epoxy Resin Treated with a Phosphorus and Silicon-containing Compound

YI CHEN, WENQIN HE, SHIQI CHEN AND JIANGBO WANG\*

*School of Materials and Chemical Engineering, Ningbo University of Technology, Ningbo, Zhejiang 315211, China*

## ABSTRACT

*In the present work, the flame retardancy and thermal degradation behavior of epoxy resin (EP) treated with a phosphorus and silicon-containing compound (DOPO-V) were investigated. Cone calorimetry measurement revealed that a significant reduction of peak heat release rate (PHRR) and total heat release (THR) of EP/DOPO-V (FREP) relative to the pure EP was achieved. Moreover, the Kissinger and Flynn-Wall-Ozawa methods were used to determine the activation energy for the degradation of pure EP and FREP composites. The kinetic results showed that the addition of DOPO-V decreased the activation energies of the first and middle stage in EP degradation and subsequently increased the activation energies in the final stage. It suggested that during the thermal degradation of FREP, the flame retardant DOPO-V induced the thermal degradation of EP matrix in a relatively lower temperature promotes the char formation. Then it restrained the thermal degradation in the final stage resulting improvement in the flame retardancy of EP composites.*

*KEYWORDS : Flame retardancy, Thermal degradation, Epoxy resin, DOPO-V, Kinetics*

## 1. INTRODUCTION

Epoxy resins (EP) have been commercialized for 70 years, owing to their satisfactory mechanical, chemical, electrical and thermal properties. Epoxy resin are widely used in diverse areas such as coatings, adhesives,

encapsulating materials, and composites<sup>[1-4]</sup>. However, the high flammability is one of the main drawbacks for EP, which greatly restricts their applications. Thus, to improve the flame retardancy of EP is increasingly the focus of many researchers' attention<sup>[5-7]</sup>.

---

J. Polym. Mater. Vol. **35**, No. 3, 2018, 329-340

© Prints Publications Pvt. Ltd.

Correspondence author e-mail : jiangbowang@163.com

DOI : <https://doi.org/10.32381/JPM.2018.35.03.7>

In recent years, halogen-free flame retardants for epoxy resins have been developed to protect the environment and human health [8-10].

Organophosphorous compounds have exhibited good flame retardancy for polymeric materials. They can form a carbonaceous char during combustion, which acts as a physical barrier to insulate heat from the flame and to prevent the diffusion of combustible gases. Therefore, flame-retardant epoxy resins can be achieved through the addition of phosphorus-containing oxiranes, and various efforts have been reported in this field. However, major problem encountered with this system is that the high loading leads to the deterioration in mechanical properties which is undesirable to fabricate high performance materials [11-14]. Reportedly, polysiloxane has also been used in epoxy modification as a promising method. For these polysiloxane modified epoxy resins, the conversion to the stable silicon dioxide under heat can form a glassy layer on the surface of the material to improve the flame retardation [15-17].

Moreover, phosphorus and silicon were demonstrated to exhibit a synergistic effect in their flame retardant behavior. These combined compositions exhibit extremely high efficiency in flame retardancy and provide an approach for reducing the amounts of flame retardant used. Consequently, the cost is reduced and thermal properties are enhanced [18-21].

In the present work, the flame retardancy and thermal stability of the prepared phosphorus and silicon-containing epoxy resin were evaluated by the cone calorimetry and TGA measurements. The kinetics and mechanism of thermal degradation of the final polymers were examined. These results revealed some

criteria for enhancing the flame retardancy of epoxy resins.

## 2. EXPERIMENTAL

### 2.1 Materials

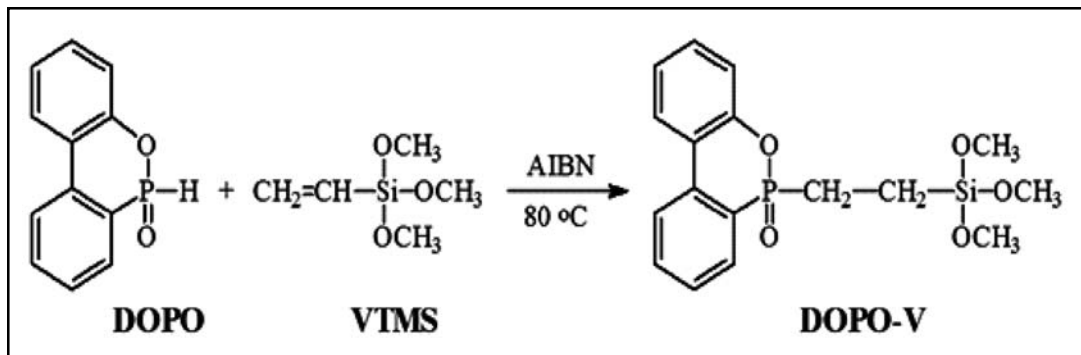
9,10-dihydro-9-oxa-10-phosphaphenanthrene-10-oxide (DOPO) was purchased from TCI Development Co., Ltd. Vinyltrimethoxysilane (VTMS) and benzene were reagent grade and purchased from Sigma-Aldrich Co., Ltd. 2,2'-Azobisisobutyronitrile (AIBN) was purchased from Alfa Aesar Chemical Reagent Co. Ltd. EPON 826 with an epoxy equivalent weight of 178-186 grams was supplied by Hexion and used as received. The hardener, Jeffamine D230, with an amine equivalent weight of 60 grams, was supplied by Huntsman Corp. and used as received.

### 2.2 Synthesis of DOPO-V

DOPO (21.6 g, 0.1 mol), VTMS (14.8 g, 0.1 mol), and benzene (100 mL) were added into a three-necked flask with a mechanical stirrer, flux condenser, dropping funnel, and nitrogen inlet. After the mixture was saturated with nitrogen atmosphere under vigorous mechanical stirring, the temperature was warmed to 80 °C. After the DOPO was dissolved completely, 0.1 g of AIBN which was predissolved in 50 mL of benzene was slowly dropped into the above reaction vessel within 2 h at 80 °C and then kept at that temperature for 24 h. After that, the products were purified by filtering. Then benzene was removed by a rotary evaporator, yielding a colorless liquid product named DOPO-V [22].

### 2.3 Preparation of epoxy composites

Briefly, the EP/DOPO-V (FREPE) composite was prepared as follows: The DOPO-V (5 g) was added into EPON 826 (71.25 g) and dispersed by a mechanical stirrer for 30 min. Subsequently, D230 (23.75 g) was added into the mixture and stirring for 30 min. After degassed in vacuum for 10 min to remove any trapped air, the sample was cured at 80 °C for 2 h and post cured at 135 °C for 2 h. For comparison, pure EP was also prepared at same processing condition.



Scheme 1. The synthesis of DOPO-V

#### 2.4 Characterization and measurement

FTIR spectra of the dried samples were recorded using a Broker Equinox-55 IR spectrometer at a resolution of  $2\text{ cm}^{-1}$  with 20 scans. The samples were mixed with potassium bromide and pressed to a disc, which was used to measure. Dynamic mechanical thermal analysis (DMA) was determined using a Rheometric Scientific SR-5000 dynamic mechanical analyzer. Data were collected from  $40\text{ }^{\circ}\text{C}$  to  $140\text{ }^{\circ}\text{C}$  at a scanning rate of  $5\text{ }^{\circ}\text{C}/\text{min}$ . Cone calorimeter measurement was performed on an FTT cone calorimeter (Britain) according to ASTM E1354 with heat flux of  $50\text{ kW}/\text{m}^2$ . The dimensions of each specimen was  $100\times 100\times 3\text{ mm}^3$ . The limiting oxygen index (LOI) was measured on an oxygen index instrument JF-3 produced by Jiangning Analysis Instrument Factory and performed according to GB2406-93. Thermogravimetric analysis (TGA) was carried on a TA instrument Q5000 thermogravimetric analyzer. The sample (about 10 mg) was heated from  $50\text{ }^{\circ}\text{C}$  to  $600\text{ }^{\circ}\text{C}$  at a set heating ramp rate in nitrogen atmosphere.

#### 2.5 Thermal degradation theory

The kinetics of thermal transformation of a solid state chemical reaction is generally based on the assumption that the reaction rate is:

$$r = \frac{da}{dt} = kf(a) \quad (1)$$

where  $f(a)$  is the reaction model,  $a$  the degree of conversion,  $k$  the temperature dependent rate constant,

$t$  the time and  $r$  the rate of degradation.  $k$  is normally assumed to obey the Arrhenius equation:

$$k = A \exp(-E / RT) \quad (2)$$

where  $E$  is the activation energy of the kinetic process,  $A$  the pre-exponential factor,  $T$  the temperature and  $R$  the universal gas constant.

Then, the rate of degradation, which is dependent on the temperature and the weight change of the sample, can be expressed as:

$$\frac{da}{dt} = Af(a) \exp(-E / RT) \quad (3)$$

Eq. (3) is also used in its integral form, which for isothermal conditions becomes

$$\ln t = E / RT - \ln[A / g(x)] \quad (4)$$

For non-isothermal degradation, Eq. (3) becomes

$$\frac{da}{dT} = (A / \beta) f(a) \exp(-E / RT) \quad (5)$$

Where,  $\beta$  is the heating rate ( $\beta = \frac{dT}{dt}$ ),  $g(x)$  is the

integrated forms of mechanism ( $g(x) = \int_0^a \frac{da}{f(a)}$ ).

1) Kissinger method<sup>[23]</sup>

The Kissinger expression is as follows:

$$\ln\left(\frac{\beta}{T_{\max}^2}\right) = \ln\left(\frac{AR}{E}\right) - \frac{E}{RT_{\max}} \quad (6)$$

where  $T_{\max}$  is the temperature of the peak rate.

The peak rate temperatures determined at different heating rates allow the activation energy to be calculated by the Kissinger method. Plotting the natural logarithm of  $\ln(\beta/T_{\max}^2)$  against the reciprocal of the absolute temperature ( $1/T_{\max}$ ), the slope of the resulting line is given by  $-E/R$ , which allows the value of  $E$  to be obtained.

## 2) Flynn-Wall-Ozawa method [24-25]

The equation of Flynn-Wall-Ozawa method can be expressed as follows:

$$\lg(\beta) = \lg AE / g(a)R - 2.315 - 0.457 \frac{E}{RT} \quad (7)$$

The above equation shows that  $\lg(\beta)$  is linearly proportional to  $1/T$ . The activation energy for any particular degree of degradation can then be

determined by a calculation of the slope from the  $\lg(\beta) - 1/T$  plots.

## 3. RESULT AND DISCUSSION

### 3.1 FTIR

The chemical structure of DOPO-V was characterized by FTIR spectra and shown in Figure 1. The peaks at 1275 and 922  $\text{cm}^{-1}$  corresponded to the stretching vibrations of P=O and P-O-C, and the peak at 1478  $\text{cm}^{-1}$  belong to the stretching vibrations of P-Ph. Moreover, the characteristic peak for Si-OH and C-H could be observed at 3429 and 3069  $\text{cm}^{-1}$ , respectively. The strong absorption bands between 1200-1000  $\text{cm}^{-1}$  indicated the existence of Si-O-C and Si-O-Si bonds. The disappearance of the absorbance peak in the region around 2436  $\text{cm}^{-1}$ , which was characteristic of P-H group of DOPO, also confirmed the successful synthesis of DOPO-V.

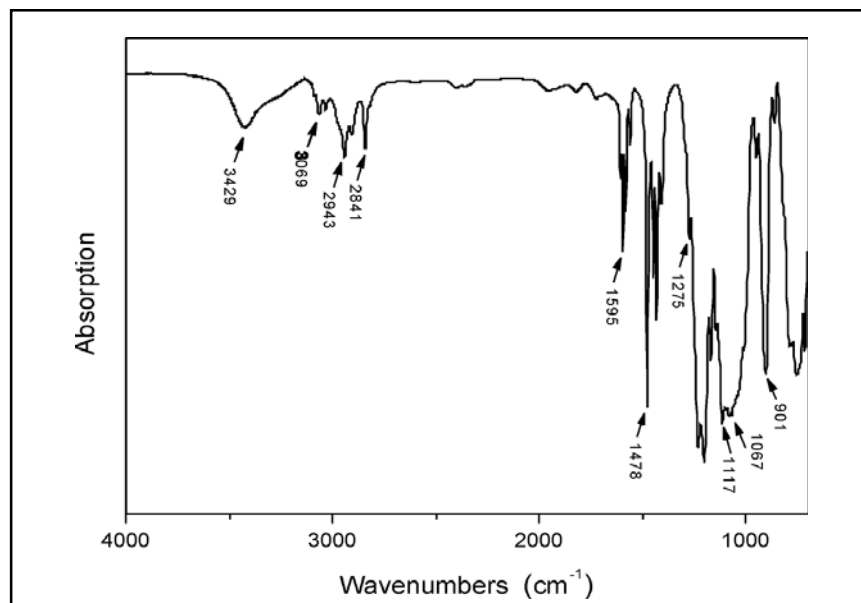


Fig. 1. FTIR spectra of DOPO-V

### 3.2 Flame retardancy

As shown in Fig. 2, the flame retardancy of EP/DOPO-V composites was investigated by the LOI measurement. It was obtained that the LOI value of pure EP was only 19.2%. With

the incorporation of 9 wt% DOPO-V, the LOI value of EP was increased to 26.8%. Compared with existing flame retardants (especially pure silicone), the flame-retardant efficiency of DOPO-V was higher than them [26].

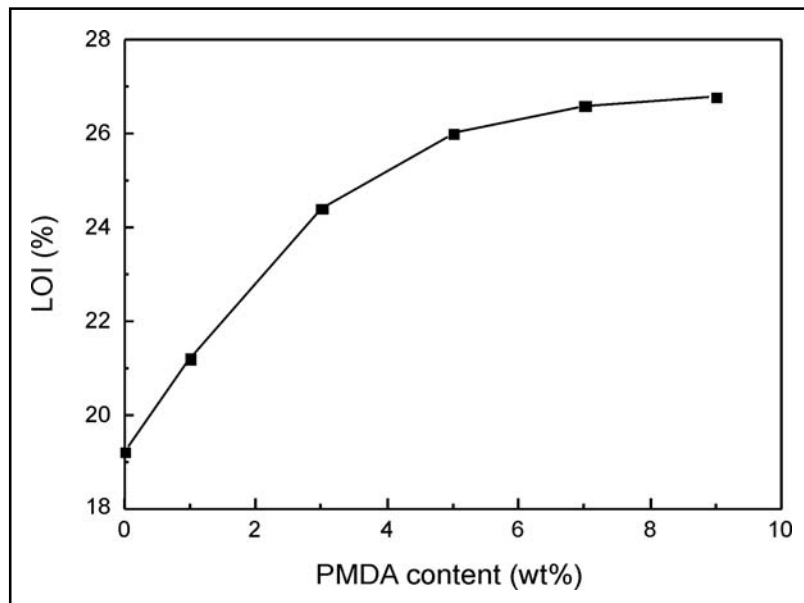


Fig. 2. The LOI of EP composites

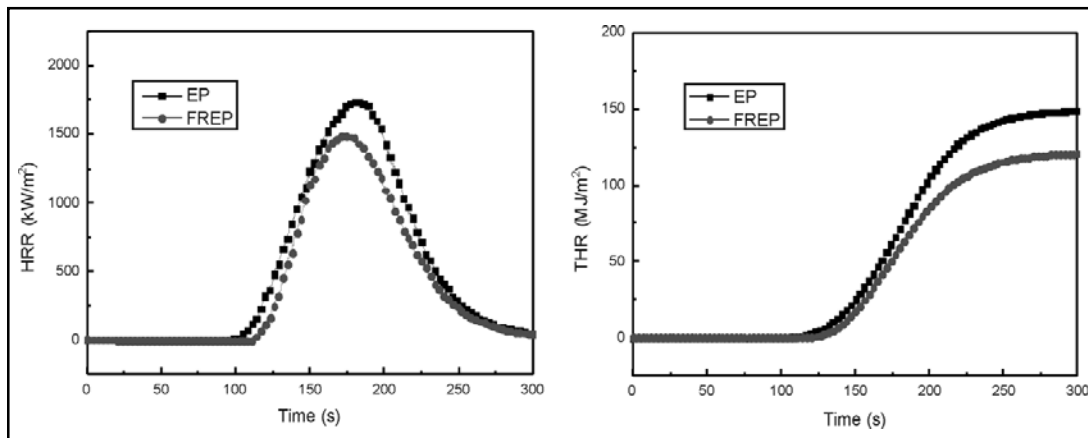


Fig. 3. HRR and THR curves of EP composites

The cone calorimeter is one of the most important bench-scale methods for studying the flame retardancy of polymeric materials. Fire-relevant properties such as the heat release rate (HRR) and total heat release (THR) are vital to the evaluation of the fire safety of materials. Fig. 3 illustrated HRR and THR curves of EP composites. As the curves showed, pure EP burned rapidly after ignition and peak heat release rate (PHRR) reached 1742 kW/m<sup>2</sup>. The HRR value of FREP decreased to a great extent compared with pure EP, of which PHRR reached 1496 kW/m<sup>2</sup>. Moreover, the THR of FREP was also reduced compared with pure EP. These results

confirmed that the DOPO-V could act as an attractive flame retardant for EP.

### 3.3 Mechanical properties

The mechanical properties of EP and the FREP composites were evaluated by the DMA tests as shown in Fig. 4. According to the storage modulus and tan delta curves of EP and FREP composites, the storage modulus of EP was decreased by the addition of DOPO-V, which could be interpreted from the change of tan delta. From the Fig.4(b), the double peaks of FREP was emerged, which was caused by the microphase separation between EP matrix and DOPO-V.

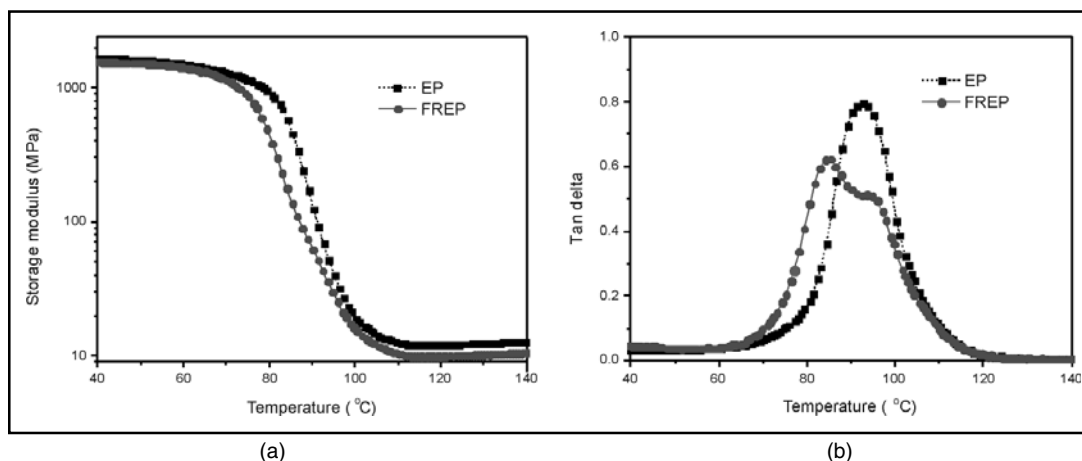


Fig. 4. Storage modulus (a) and tan delta (b) curves for EP and FREP in the DMA test

### 3.4 Thermal stability

Fig. 5 showed TGA and DTG curves of EP and FREP composites under nitrogen atmosphere. The related data of the onset degradation temperature ( $T_{5wt\%}$ ), the temperature at maximum degradation rate ( $T_{max}$ ) and the residual char at 600°C obtained from the curves were summarized in Table 1. The TGA curves

exhibited that by introducing DOPO-V into EP matrix, the onset thermal degradation temperature was lower compared with pure EP. Moreover, the  $T_{max}$  was also decreased gradually with the addition of the flame retardant DOPO-V. It was due to the early degradation of phosphorus-containing group in DOPO-V structure and subsequently induced the thermal

degradation of EP matrix in a relatively lower temperature, which prevented the further degradation of the epoxy matrix.

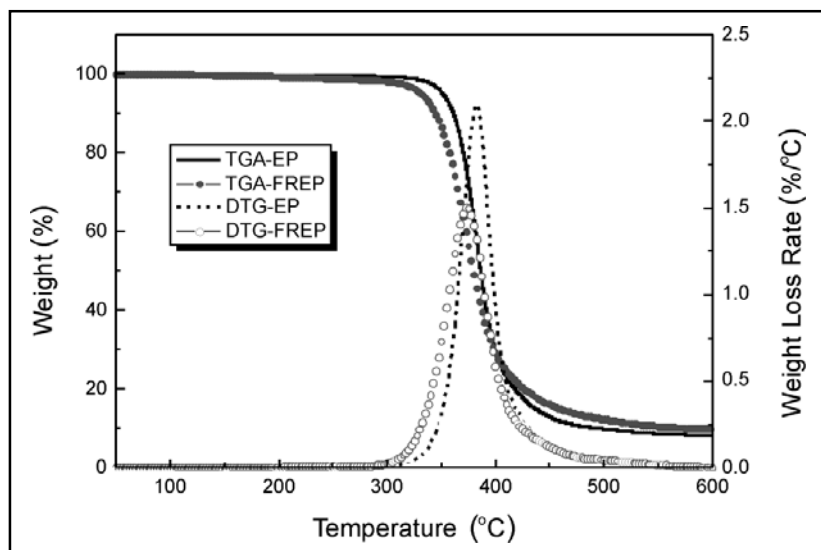


Fig. 5. Thermal stability of EP composites

TABLE 1. TGA data of EP composites

	Temperature (°C)		Peak rate(wt%/°C)	Residual char(wt%)
	$T_{5wt\%}$	$T_{max}$		
EP	351.7	382.6	2.10	8.27
FREP	331.7	373.2	1.51	10.07

However, the residual char of FREP arrived at 10.07 wt%, which was obviously higher than 8.27 wt% of pure EP. The reasonable explanation was attributed to the fact that the synergistic effect of phosphorus/silicon on the char formation of EP was noteworthy, and the high thermal stability of the formed char at high temperature regions was achieved. The charred layer accumulated on the surface of the material and acted as a protective barrier to inhibit the flame and heat transfer of the

underlying substance, endowing a significant enhancement in the flame retardancy<sup>[27]</sup>.

### 3.5 Thermal degradation kinetics

The TGA and corresponding DTG curves of dynamic thermal degradation of EP and FREP obtained in the temperature range 50-600 °C at the heating rates of 5, 10, 20 and 40°C/min were shown in Fig. 6. It was evident that the thermal degradation of pure EP and FREP proceed by a one-step process between 300

and 500°C, which was represented by a single peak in the corresponding DTG curves. It was clear that with the increase of heating rate,

the degradation of EP composites started at higher temperature and the temperature at the maximum rate of EP degradation increased.

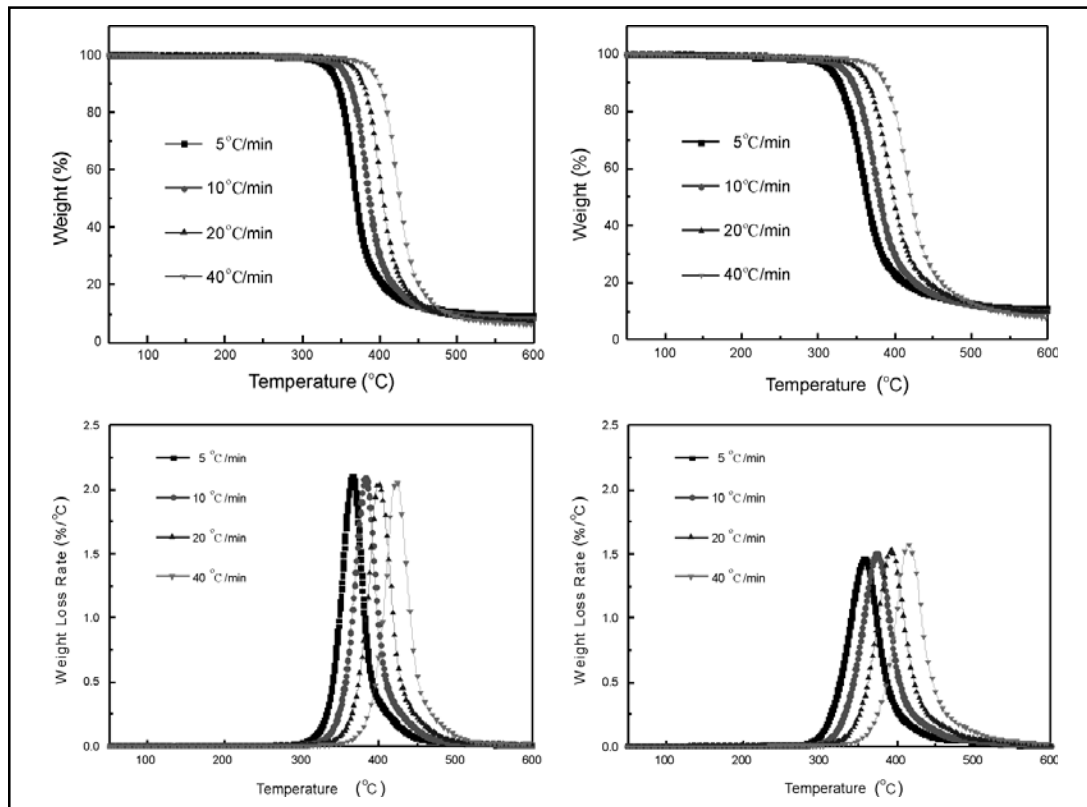


**Fig. 6.** TGA and DTG curves of EP composites

In this study, the TGA and DTG curves of EP composites at different heating rates were used to calculate the kinetic parameters of thermal degradation process by the Kissinger and Flynn-Wall-Ozawa methods. These two methods could be derived from a common fundamental kinetic equation for heterogeneous chemical reactions, and therefore had common features, i.e. wide applicability and high reliability.

According to the Kissinger method, the activation energy of thermal degradation could be obtained by plotting  $(\beta/T_{\max}^2)$  versus  $(1/T_{\max})$  for all heating rates used, as shown in Fig. 7. Using Kissinger method could get good linear regression, which could accurately calculate the activation energy value and kinetic parameter values and so on. Their  $E$  values calculated based on Eq. (6) from Kissinger method were listed in Table 2. It could be seen

that the degradation activation energy of FREP (122.1 kJ/mol). It was possibly due to the was 120.1 kJ/mol, lower than that of pure EP degradation of DOPO-V.

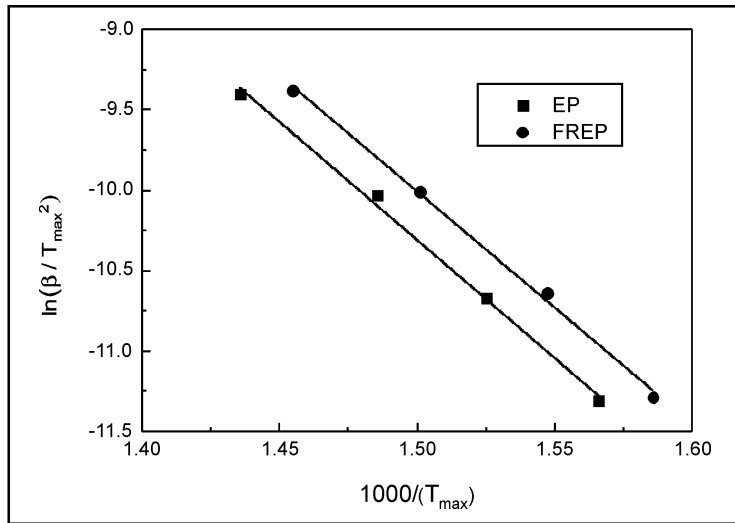


Fig. 7. The curves  $\ln(\beta/T_{max}^2)$  vs.  $(1/T_{max})$  of EP and FREP

TABLE 2. Kinetic data for degradation of EP and FREP by Kissinger method

	$T_{max}$ (°C)				$E$ (kJ/mol)	$\ln A$ (1/min)
	5°C/min	10°C/min	20°C/min	40°C/min		
EP	365.4	382.6	400.1	423.5	122.1	14.4
FREP	357.5	373.2	393.0	414.3	120.1	14.3

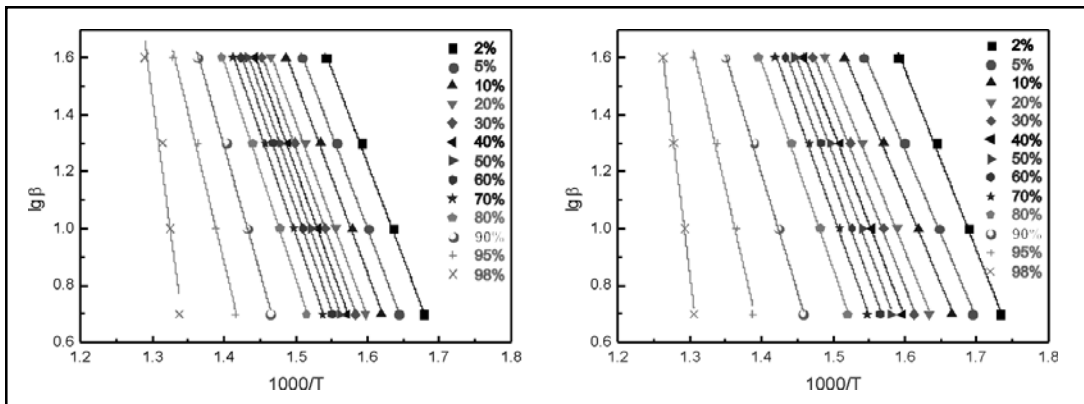


Fig. 8. The curves of  $\lg(\beta)$  vs.  $1/T$  of EP and FREP

Flynn-Wall-Ozawa model is another widely used method to calculate activation energy of solid phase. According to the Eq. (7),  $E$  is obtained from the slope of the straight line in relation to a plot of  $\lg(\beta)$  versus  $1/T$  at a fixed conversion  $\alpha$ . Fig. 8 plotted the logarithm of heating rate ( $\beta$ ) against reciprocal absolute temperature ( $T$ ) of EP and FREP.

If the straight lines are parallel,  $E$  is a constant in the range of conversion, and that the degradation process is one step in the range of conversion analyzed. The activation energy values were calculated from the straight lines in Fig. 8 by the Flynn-Wall-Ozawa method, which were shown in Fig. 9.

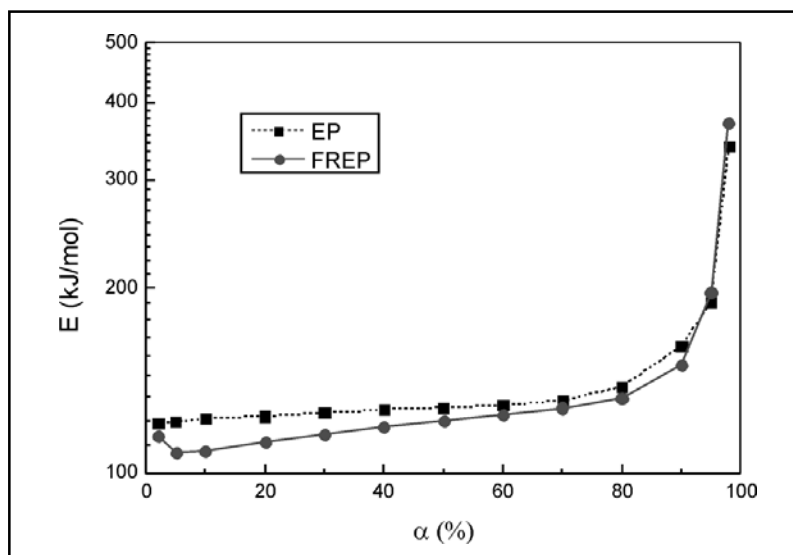


Fig. 9. Activation energy curves of EP and FREP by Flynn-Wall-Ozawa method

It could be obtained that the activation energy of pure EP was increased along with the increase of  $\alpha$ , indicating that the degradation of EP became difficult with the thermal degradation process. Moreover, in the early and middle degradation stages, the activation energy of pure EP was slightly higher than that of FREP. It indicated that the addition of DOPO-V induced the thermal degradation of EP matrix, which was agree with the results observed from the TGA and DTG curves. However, compared with the pure EP, the

activation energy of FREP was higher in the final stage ( $\alpha > 90\%$ ), which could be due to the formation of compact char layer in this stage. And it could serve as a barrier to slow down the heat and mass transfer at high temperature. The above results indicated that the phosphorus and silicon-containing flame retardant DOPO-V could promote the char formation during the thermal degradation of FREP and restrain the thermal degradation in the final stage, which greatly improved the flame retardancy of the composites.

## 5. CONCLUSION

This study successfully showed that the DOPO-V could greatly improve the flame retardancy of EP. Cone calorimetry measurement exhibited that the HRR and THR of FREP were both reduced compared with pure EP. Moreover, the methods of Kissinger and Flynn-Wall-Ozawa showed that the addition of DOPO-V decreased the activation energy of the first and middle stage in EP degradation, which suggested that during the thermal degradation of FREP, the flame retardant DOPO-V induced the thermal degradation of EP matrix in a relatively lower temperature. Subsequently, the activation energies of FREP were higher than those of pure EP in the final thermal degradation stage. It was attributed to the addition of DOPO-V, which promoted the char formation, restrained the thermal degradation in the final stage, resulting improvement in the flame retardancy of EP composites.

## Acknowledgments

The authors wish to thank the Ningbo Natural Science Foundation (2017A610067), National Undergraduate Training Program for Innovation and Entrepreneurship (201811058002), Zhejiang Provincial Innovation Training Plan for University Students (2017R424009) and Ningbo Municipal Program for Leading and Top-Notch Talents for financial support.

## REFERENCES

1. H. Gu, C. Ma, J. Gu, J. Guo, X. Yan, J. Huang, Q. Zhang and Z. Guo. *J. Mater. Chem. C*, (2016), 4, 5890-5906.
2. H. Huang, K. Zhang, J. Jiang, J. Li and Y. Liu. *Polym. Int.*, (2017), 66, 85-91.
3. X. Zhao, H.V. Babu, J. Llorca and D.Y. Wang. *RSC Adv.*, (2016), 6, 59226-59236.
4. L. Chen, S.G. Chai, K. Liu, N.Y. Ning, J. Gao, Q.F. Liu, F. Chen and Q. Fu, *Acs Appl. Mater. Inter.*, (2012), 4(8), 4398-4404.
5. E.D. Weil and S. Levchik. *J. Fire Sci.*, (2004), 22(1), 25-40.
6. S. Liu, H. Yan, Z.P. Fang and H. Wang. *Compos. Sci. Technol.*, (2014), 90, 40-47.
7. R. Jian, P. Wang, W. Duan, J. Wang, X. Zheng and J. Weng. *Ind. Eng. Chem. Res.*, (2016), 55, 11520-11527.
8. A.B. Morgan and C.A. Wilkie. *Flame retardant polymer nanocomposites*. John Wiley & Sons, (2007).
9. A. Covaci, S. Harrad, M.A.E. Abdallah, N. Ali, R.J. Law, D. Herzke and C.A. de Wit. *Environ. Int.*, (2011), 37, 532-556.
10. C.A. de Wit, D. Herzke and K. Vorkamp. *Sci. Total Environ.*, 2010, 15, 2885-2888.
11. X. Wang, W. Xing, X. Feng, B. Yu, L. Song and Y. Hu. *Polym. Chem.*, (2014), 5(4), 1145-1154.
12. Y. Liu, G. Hsiue and Y. Chiu. *J. Polym. Sci. Polym. Chem.*, (1997), 35(3), 565-574.
13. M. Rakotomalala, S. Wagner and M. Döring. *Materials*, (2010), 3(8), 4300-4327.
14. R. Ménard, C. Negrell, L. Ferry, R. Sonnier and G. David. *Polym. Degrad. Stab.*, 2015, 120, 300-312.
15. W.J. Wang, L.H. Peng and G.H. Hsiue. *Polymer*, (2000), 41, 6113-6120.
16. K. Wu, L. Song, Y. Hu, H. Lu, B.K. Kandola and E. Kandare. *Prog. Org. Coat.*, (2009), 65(4), 490-497.
17. L.A. Mercado, M. Galia, J.A. Reina. *Polym. Degrad. Stab.*, (2006), 91: 2588-2594.
18. N.J. Kang, Z.J. Du, H.Q. Li and C. Zhang. *Polym. Adv. Technol.*, (2012), 23, 1329-1334.

19. L. Zhang, Y. Wang, Q. Liu and X. Cai. *J. Therm. Anal. Calorim.*, (2016), 123(2), 1-8.
20. Y. Shi and G. Wang. *Appl. Surf. Sci.*, (2016), 385, 453-463.
21. Chao, P. Y. Li, X. Gu, D. Han, X. Jia, M.Q. Wang, T.F. Zhou and T. Wang. *Polym. Chem.*, (2015), 6(15), 2977-2985.
22. X.D. Qian, H.F. Pan, X.Y. Xing, L. Song, R. Yuen and Y. Hu. *Ind. Eng. Chem. Res.*, (2012), 51, 85-94.
23. H.E. Kissinger. *Anal. Chem.*, (1957), 29(11), 1702-1706.
24. J.H. Flynn. *J. Polym. Sci. Pol. Lett.*, (1966), 4(5), 323-328.
25. J.H. Flynn. *J. Polym. Sci. Pol. Lett.*, (1967), 5(2), 191-196.
26. J.B. Wang. *Journal of Polymer Materials*, (2018), 35(1), 33-44.
27. C.S. Wu, Y.L. Liu and Y.S. Chiu. *Polymer*, (2002), 43, 4277-4284.

Received: 10-09-2018

Accepted: 03-11-2018